BIOCHEMISTRY
including biophysical chemistry & molecular biology
Article

Biochemistry **2010,** *49,* 9385–9390 9385
DOI: 10.1021/bi1012047

Histidine 197 in Release Factor 1 Is Essential for A Site Binding and Peptide Release†

Andrew Field,‡ Byron Hetrick,‡ Merrill Mathew, and Simpson Joseph*

Department of Chemistry and Biochemistry, University of California, San Diego, 9500 Gilman Drive, La Jolla, California 92093-0314, United States ‡These authors contributed equally to this work.

Received July 29, 2010; Revised Manuscript Received September 23, 2010

ABSTRACT: Class I peptide release factors 1 and 2 (RF1 and RF2, respectively) recognize the stop codons in the ribosomal decoding center and catalyze peptidyl-tRNA hydrolysis. High-fidelity stop codon recognition by these release factors is essential for accurate peptide synthesis and ribosome recycling. X-ray crystal structures of RF1 and RF2 bound to the ribosome have identified residues in the mRNA−protein interface that appear to be critical for stop codon recognition. Especially interesting is a conserved histidine in all bacterial class I release factors that forms a stacking interaction with the second base of the stop codon. Here we analyzed the functional significance of this conserved histidine (position 197 in *Escherichia coli*) of RF1 by point mutagenesis to alanine. Equilibrium binding studies and transient-state kinetic analysis have shown that the histidine is essential for binding with high affinity to the ribosome. Furthermore, analysis of the binding data indicates a conformational change within the RF1·ribosome complex that results in a more tightly bound state. The rate of peptidyl-tRNA hydrolysis was also reduced significantly, more than the binding data would suggest, implying a defect in the orientation of the GGQ domain without the histidine residue.

The entry of a stop codon into the ribosomal A site signals the termination phase of protein synthesis. The nearly universally conserved stop codons UAA, UAG, and UGA are recognized by class I release factors (RFs)[1] (*1*). In bacteria, there are two class I release factors: RF1 and RF2. RF1 recognizes UAA and UAG, while RF2 recognizes UAA and UGA (*2*). In eukaryotes, a single class I release factor, eRF1, recognizes all three stop codons (*3*). Following the recognition of the stop codon in the A site, class I release factors trigger peptidyl-tRNA hydrolysis and the release of the newly synthesized protein from the ribosome (*4*). Accurate recognition of stop codons by RFs is essential to prevent premature termination, which would be costly to the cell. The fidelity of stop codon recognition by RFs has been estimated to be 1×10^{-3} to 1×10^{-6} (*5*, *6*), which is arguably more accurate than tRNA selection on cognate codons. Remarkably, this high level of accuracy in stop codon recognition is achieved by RFs without the help of a proofreading mechanism.

Previously, the kinetics of RF1 and RF2 discrimination between stop and sense codons were systematically analyzed under steady-state conditions (*6*). These studies showed that a sense codon in the decoding center increases the K_M between the release factors and the ribosome by 400−3000-fold, while the catalytic rate constant for peptide release (k_{cat}) was reduced by 2−180-fold (*6*). Thus, discrimination seems to be achieved by the RFs mainly at the binding step. However, binding was not measured directly (K_M is not equal to K_D), and changes in k_{cat} may also occur with improper placement of the RFs in the ribosome.

More recently, the binding of RF1 to ribosomes with stop or sense codons in the decoding center was directly measured using a fluorescence-based, pre-steady-state kinetic assay (*7*). These studies showed that the association rate constant of RF1 with the ribosome is similar with both sense and stop codons, while the dissociation rate constant increased by as much as 4000-fold when a sense codon is present in the decoding center. Furthermore, defects in RF1 binding to the ribosome do not always correlate with a reduced rate of peptide release, suggesting that conformational changes in the ribosome·RF complex occur prior to catalysis (*7*).

A conserved "anticodon tripeptide" motif (PXT in RF1 and SPF in RF2) that is important for the specificity of stop codon recognition was identified by genetic analysis (*8*). More recent X-ray crystal structures of RF1 or RF2 bound to the ribosome have shown additional residues that may also be used for stop codon recognition (*9*−*11*). Strikingly, in both RF1 and RF2, the imidazole ring of a conserved histidine (residues 193 and 203 of *Thermus thermophilus* RF1 and RF2, respectively) is inserted between the second and third base of the stop codon (*9*, *10*) (Figure 1). The second base makes a stacking interaction with His 193/203, while the third base rearranges and stacks on G530 of 16S rRNA. Unstacking of the third base distorts the mRNA backbone causing A1492 of 16S rRNA to move out from helix 44 and contact the mRNA backbone. Movement of A1492 opens up space for A1913 of 23S rRNA to stack with A1493 of 16S rRNA. Without these conformational changes, A1913 would block binding of RFs. Thus, His 193/203 seems to play a key role in switching the conformation of the ribosome to a state that is

†This work was supported by National Institutes of Health (NIH) Molecular Biophysics Training Grant GM08326 and NIH Training Program in Hemoglobin and Blood Protein Chemistry Grant 5T32-DK007233 to B.H. and NIH Grant GM065265 to S.J.

*To whom correspondence should be addressed: 4102 Urey Hall, Department of Chemistry and Biochemistry, University of California, San Diego, 9500 Gilman Dr., La Jolla, CA 92093-0314. Phone: (858) 822-2957. Fax: (858) 534-7042. E-mail: sjoseph@ucsd.edu.

[1]Abbreviations: RF, release factor; rRNA, ribosomal RNA; mRNA, messenger RNA; tRNA, transfer RNA.

Published on Web 09/28/2010

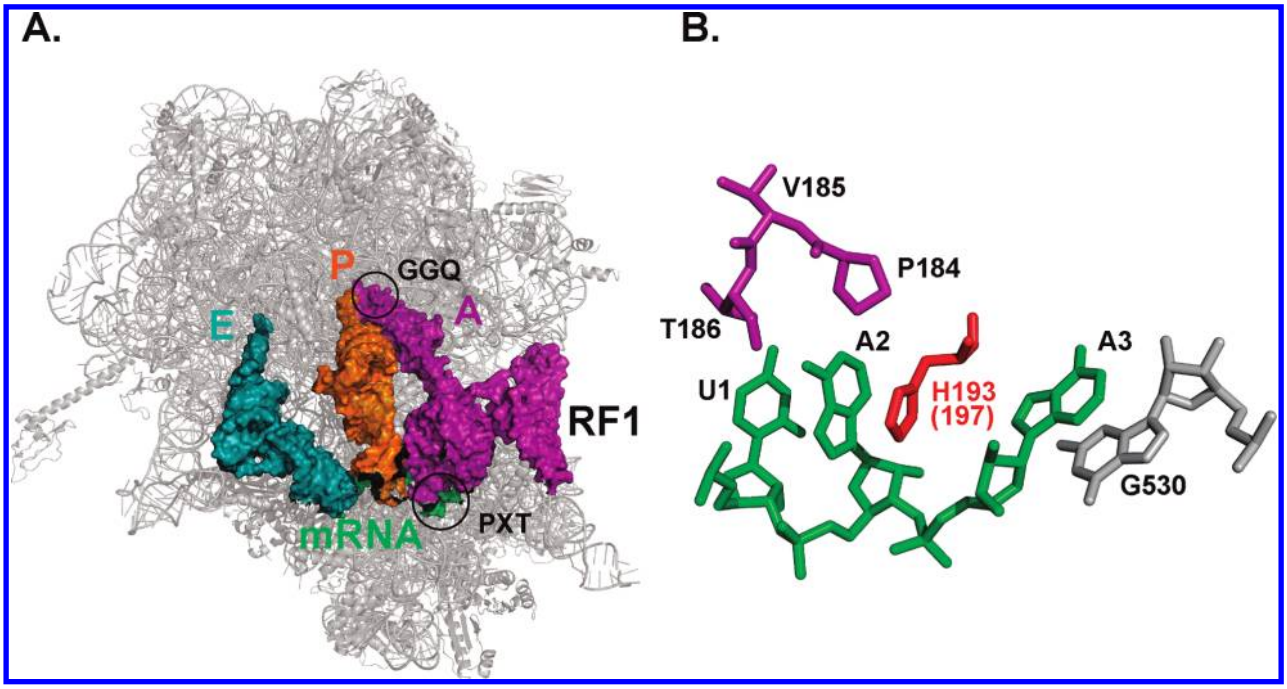

FIGURE 1: Structure of RF1 bound to the ribosome. (A) Location of RF1 in the ribosome: ribosome (gray), RF1 (purple), P site tRNA (orange), E site tRNA (teal), and mRNA (green). Circles indicate the highly conserved GGQ and PXT loops. (B) Close-up of the interactions between RF1 and the stop codon: RF1 residues (purple), stop codon $U_1A_2A_3$ (green), and G530 of 16S rRNA (gray). *T. thermophilus* numbering is used for the RF1 residues except for His 193 (red) where the corresponding *E. coli* residue His 197 is indicated. The structures were prepared using PyMol.

productive for RF1 and RF2 binding and peptide release. Here we analyzed the functional importance of the conserved His 197 in RF1 of *Escherichia coli* (corresponding to His 193 and His 203 of *T. thermophilus* RF1 and RF2, respectively) using equilibrium binding studies, transient-state kinetic methods, and peptide release assays. Our results show that His 197 in RF1 is critical for stably binding the release factor to the ribosome and for efficient peptide release.

EXPERIMENTAL PROCEDURES

Buffers, Ribosomes, tRNA, mRNA, and RF1 Preparation. Experiments were performed in 20 mM Hepes-KOH (pH 7.6), 150 mM NH_4Cl, 6 mM $MgCl_2$, 4 mM β-mercaptoethanol, 2 mM spermidine, and 0.05 mM spermine (*12*). *E. coli* MRE600 cells were used to produce tightly coupled 70S ribosomes as described previously (*13*). mRNA with a UAA stop codon was purchased from Dharmacon, and pyrene was covalently attached as described previously (*14*). Native $tRNA^{fmet}$ was purchased from Sigma. His-tagged *E. coli* RF1 (termed wild type from here on) was purified as described previously (*7*).

Mutant H197A RF1. QuickChange (Stratagene) site-directed mutagenesis was utilized to produce the H197A RF1 mutant from the wild-type RF1 plasmid. DNA primers for the mutation were purchased from ValueGene. H197A RF1 was then sequenced, transformed into BL21(DE3), and purified in the same manner as wild-type RF1.

Fluorescence Measurements and K_D Titrations. Release complexes were formed as described previously (*7*). The final concentrations of the release complex were 50 and 5 nM for H197A and wild-type RF1 experiments, respectively. The indicated amounts of RF1 were added to the ribosome mixtures and incubated at room temperature for at least 5 min prior to fluorescence measurement. The fluorescence of the ribosome complexes was measured on a Fluoromax-P instrument (J. Y. Horiba, Inc.) with an excitation and emission bandpass of 1 nm and an excitation wavelength of 343 nm, and emission at 376 nm was recorded. Experiments were preformed in triplicate. Normalized emission changes were fit using Graphpad Prism using the equation below as described previously (*7*).

$$Y = m\{K + R + X - [(K+R+X)^2 - 4RX]^{1/2}\}/(2R)$$

where Y is the fluorescence, X is the concentration, m is the maximal fluorescence signal, K is the dissociation constant (K_D), and R is the 70S ribosome concentration.

Stopped-Flow Binding Kinetics. Stopped-flow measurements were performed essentially as described previously (*7*). Time courses were performed with 0.25 μM release complex and the indicated amount of RF1. Data were fit to the second-order rate equation

$$Y = b + C_1 \exp(-k_1 x) + C_2 \exp(-k_2 x)$$

where C_1 and k_1 are the amplitude and rate, respectively, for phase 1 and C_2 and k_2 are the amplitude and rate, respectively, for phase 2.

Peptide Release Assay. 70S ribosomes (final concentration of 0.50 μM) were incubated at 42 °C for 10 min and then cooled to 37 °C for 10 min. mRNA (final concentration of 1 μM) was added to the 70S and incubated at 37 °C for an additional 10 min. $tRNA^{fmet}$ was charged as described previously (*7*) and added to the 70S−mRNA complex for a final tRNA concentration of 1.5 μM. This mixture was then incubated at 37 °C for 30 min. Excess [^{35}S]Met and other unbound reaction components were removed by repeated filtration through an Amicon Ultra 100K Ultracel centrifugal filter for a final dilution of >200000-fold. The final volume of the reaction mixture was then adjusted to a final 70S ribosome concentration of 0.50 μM. Time courses for peptide release were determined using 0.25 μM release complexes and 20 μM RF1 (both wild type and H197A). Each time point was quenched using 25% formic acid, run on an eTLC plate, and

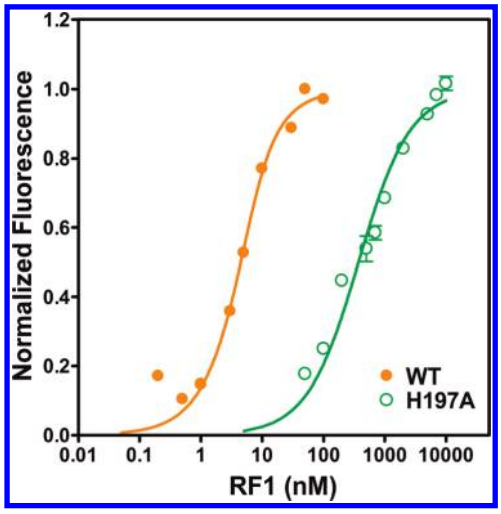

FIGURE 2: Fluorescence assay for determining the K_D of H197A RF1. Normalized changes in fluorescence intensity after the addition of increasing concentrations of wild-type RF1 (orange) or H197A RF1 (green) are shown. A representative titration experiment for wild-type RF1 without standard deviations is shown. The standard deviations from four independent experiments are shown for H197A RF1. The curves shown are fit to the quadratic equation.

analyzed as described previously (*15*). Peptide release experiments were repeated four times.

RESULTS

Equilibrium Binding of H197A RF1 to the Ribosome. To study the functional role of the highly conserved histidine at position 197 in *E. coli* RF1, we changed it to an alanine by site-directed mutagenesis. Wild-type and H197A RF1 were purified and then were analyzed for their ability to bind to ribosomes using a recently described fluorescence-based assay (*7*). Release complexes (RC) were formed by sequentially adding pyrene-labeled mRNA and $tRNA^{fMet}$ to 70S ribosomes. Binding of $tRNA^{fMet}$ to the P site positions the UAA stop codon in the A site. Increasing amounts of wild-type or H197A RF1 were added to a fixed concentration of the RC. The increase in fluorescence emission intensity due to RF1 binding to the RC was measured for each concentration of RF1. As reported previously, the affinity of wild-type RF1 for a UAA stop codon is very high (*7*). For sufficient signal to noise, the minimum concentration of RC required for the titration experiment is 5 nM, which is close to the K_D of wild-type RF1 binding to the ribosome, and hence, the K_D could not be accurately determined for wild-type RF1; our best estimate is that it is below 3 nM (Figure 2). In contrast, H197A RF1 showed an at least 100-fold increase in the K_D compared to that of wild-type RF1 ($K_D = 350 \pm 30$ nM). Thus, histidine 197 of RF1 is essential for binding to the ribosome with high affinity.

Kinetics of H197A RF1 Binding to the Ribosome. To determine the rates of stop codon recognition by RF1, we studied the transient-state kinetics of H197A RF1 binding to the RC. Time courses for RF1 binding to the RC were determined using a stopped-flow instrument (Figure 3A). A biphasic increase in fluorescence was observed when both wild-type and H197A RF1 bind to RC. Previously, the fluorescence change observed when wild-type RF1 bound to the RC was described as having only a single phase (*7*). These previous data were analyzed up to six half-lives and fit well to a single-exponential equation; however, our analysis of longer time courses revealed a second, slower phase. The simplest interpretation of the biphasic kinetic data is a two-step binding process (*16*). The first phase is likely a second-order association step and the second phase a conformational rearrangement of the complex. The observed rates of each phase of the fluorescence change were determined by fitting stopped-flow time courses to a double-exponential equation. A plot of the observed rate of the first phase of the fluorescence change versus RF1 concentration revealed a linear concentration dependence, consistent with a second-order association step (*16*) (Figure 3B). The slope of the line is the second-order association rate constant of RF1 for the ribosome (k_1). Wild-type and H197A RF1 bind to the ribosome with nearly identical association rate constants of 55 and 71 μM^{-1} s^{-1}, respectively. Therefore, the association rate constant (k_1) for RF1 binding to the ribosome was unaffected by the H197A mutation.

The dissociation rate constant (k_{-1}) was obtained from the *y*-intercept of the concentration dependence plot of phase 1 (*16*) (Figure 3B). The k_{-1} value for wild-type RF1 is very small and cannot be accurately determined, which is consistent with an equilibrium K_D of < 3 nM. Interestingly, the k_{-1} value for H197A is 175 s^{-1}, indicating that it forms an initial labile complex with the ribosome compared to wild-type RF1. The equilibrium dissociation constant for the first step in the binding reaction of H197A to the RC (K_{D1}), calculated from k_1 and k_{-1} values, is 3 μM (Figure 4B). This value is 10-fold higher than the equilibrium K_D for the overall binding reaction determined from the titration experiments described above ($K_D = 0.35 \pm 0.03$ μM). This suggests that the initial labile complex formed by H197A on the ribosome undergoes a conformational change over time to a more stable complex, further indicating a two-step binding process. Examination of the amplitudes for phase 1 is also consistent with this interpretation. The amplitude for phase 1 did not change with increasing concentrations of wild-type RF1, showing that binding has been saturated (Figure 3C), which matches the K_D for wild-type RF1 of < 3 nM. In contrast, the amplitude for phase 1 increased with increasing concentrations of H197A RF1, showing that saturation has not been reached at the lower concentrations (Figure 3C). With increasing concentrations, more H197A RF1 populates the first binding step, resulting in a greater fluorescence change and consistent with the calculated value of 3 μM for K_{D1} for H197A RF1. These results show that the H197A mutation in RF1 significantly reduces the stability of the initial complex formed on the ribosome.

The observed rates of the second phase of the fluorescence change did not vary with the concentration of RF1 for the wild type or H197A (Figure 3D). The lack of concentration dependence is consistent with a first-order conformational change after binding (*16*). The rate of the second phase of the fluorescence change is saturated at 1.3 s^{-1} for wild-type RF1 and somewhat more slowly at 0.7 s^{-1} for H197A RF1. Because the rates for the second phase are similar, it means that H197 is not critical for this conformational change to occur after the initial binding step. However, H197 is required for the stability of the complex in the second phase because the equilibrium K_D for H197A RF1 is at least 100-fold higher than that of wild-type RF1. Thus, equilibrium binding studies and kinetic analysis reveal that H197 is critical for the initial binding step and for the overall stability of RF1 in its final bound conformation on the ribosome.

Kinetics of Peptide Hydrolysis by H197A RF1. To investigate whether histidine 197 of RF1 is important for the catalytic step, the rate of peptide release by H197A RF1 was determined. Release complexes were formed by binding of

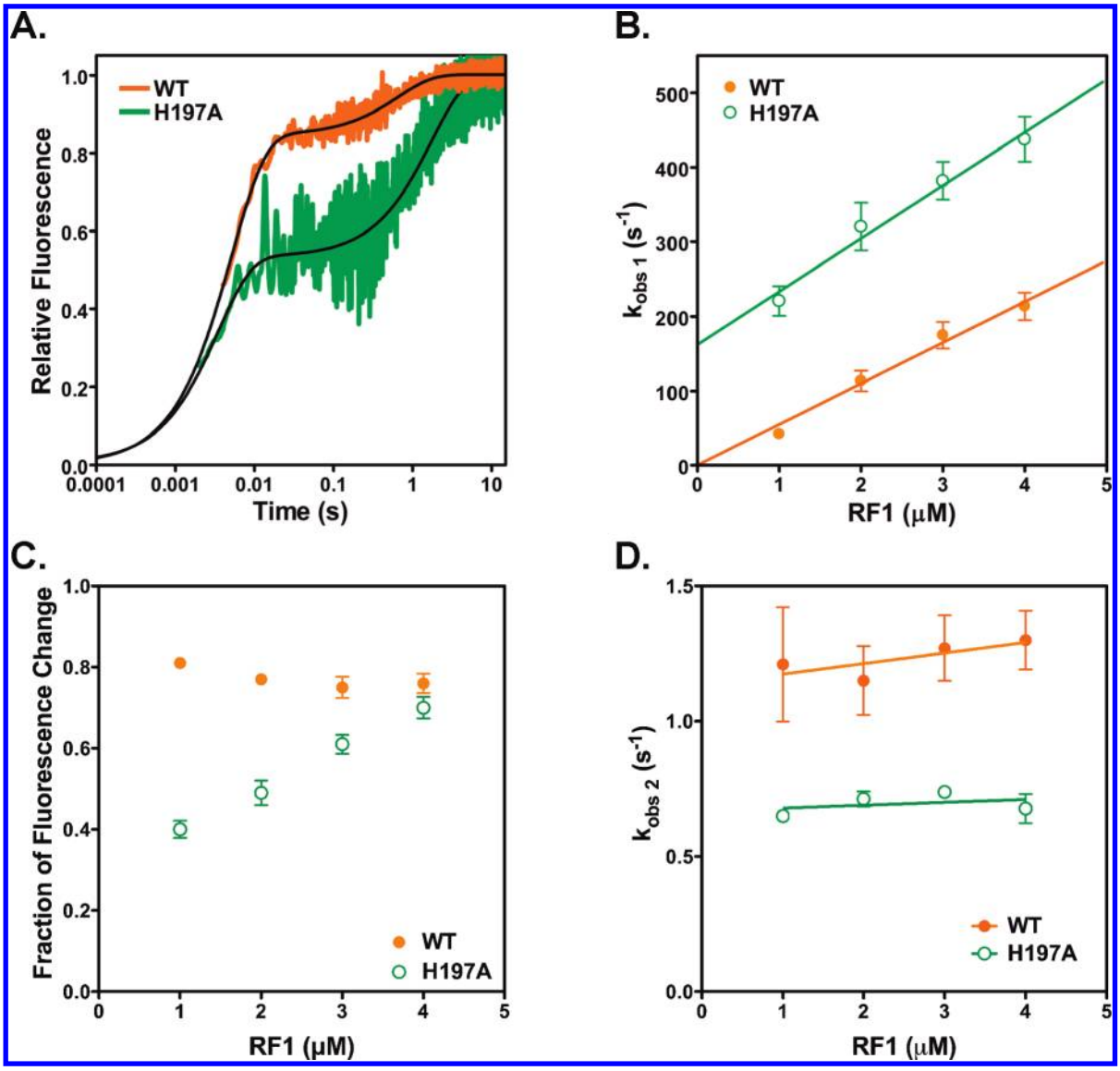

FIGURE 3: Kinetics of H197A RF1 binding to the ribosome. (A) Representative stopped-flow time course of wild-type RF1 (orange trace) and H197A RF1 (green trace) binding to the ribosome. The time courses were fit to a double-exponential equation (black line) to determine the observed rates of RF1 binding (k_{obs1} and k_{obs2}). (B) Concentration dependence of the observed rate for phase 1 of RF1 binding. Plots were fit to a linear equation to determine the association (k_1) and dissociation (k_{-1}) rate constants. (C) Concentration dependence of the amplitude for phase 1 of RF1 binding. (D) Concentration dependence of the observed rate for phase 2 of RF1 binding. Plots were fit to a linear equation. In all cases, the standard errors from at least three independent experiments are shown.

[^{35}S]fMet-tRNA^{fMet} to the P site. Peptide release time courses were performed via addition of saturating amounts of RF1 (20 μM, which is more than 50-fold above the K_D for H197A RF1 binding to RC). RF1-catalyzed release of [^{35}S]fMet was analyzed by electrophoretic TLC and quantitated with a phosphorimager. To verify that saturation was reached, we repeated the time courses with double the concentration of RF1 and obtained identical time courses. Wild-type RF1 catalyzed peptide release with a rate of $0.25 \pm 0.02\ s^{-1}$, which is consistent with previously published data (*7*, *17*). In contrast, H197A RF1 exhibited an ≈5-fold reduced rate of peptide release ($k_{release} = 0.053 \pm 0.004\ s^{-1}$). The reduced catalytic activity of H197A RF1, even under saturating concentrations, can be explained by a misalignment of the mutant RF1 in the ribosome, which may affect the positioning of the universally conserved GGQ loop in the peptidyl transferase center. Perturbations in the decoding center are known to affect the position of RF1 in the ribosome and inhibit peptide release (*17*, *18*).

DISCUSSION

Stop codon recognition by RFs is essential for the correct termination of protein synthesis in all organisms. Recent crystallographic structures have revealed the interactions between conserved residues in the RFs and the stop codon in the decoding center that are important for discrimination (*9*, *10*). These structures have also made it possible to perform molecular dynamics simulations to understand the energetics of stop codon recognition (*19*). Nevertheless, the contribution of critical residues in the RF to binding, conformational changes, and catalysis has to be determined experimentally to fully understand the mechanism of stop codon recognition.

In this study, we focused on the highly conserved His 197 in *E. coli* RF1 that seems to play a central role in triggering conformational changes in the decoding center. We made use of a recently developed fluorescence-based, transient-state kinetic method (*7*) to quantitatively evaluate the role of His 197 in stop codon recognition and in the catalysis of peptide

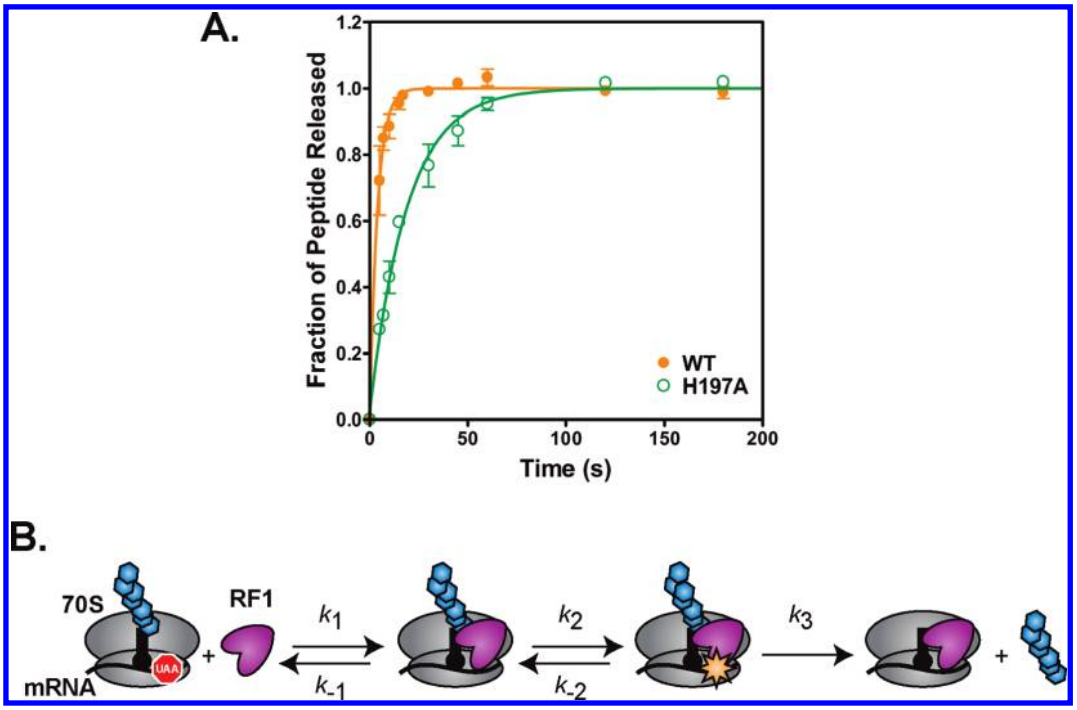

FIGURE 4: Peptide release time course and a schematic model for RF1 binding and peptide release. (A) Peptide release time courses at saturating concentrations of wild-type RF1 (orange circles) and H197A RF1 (green circles). Data were normalized and fit to a single-exponential equation (line) to determine the rate of peptide release. (B) Cartoon showing the kinetic steps in binding of RF1 to the ribosome and catalysis of peptide release. Ribosome (gray), stop codon (red), P site tRNA (black stem loop), polypeptide (blue hexagons), and RF1 (purple). Step 1 is the second-order association of RF1 with the ribosome (k_1 and k_{-1}). Step 2 is a first-order conformational switch to a more tightly bound complex (k_2 and k_{-2}). Step 3 is the peptidyl-tRNA hydrolysis reaction catalyzed by RF1 (k_3).

release. Equilibrium binding studies showed that H197A RF1 has a significantly larger K_D that is 100-fold greater than that of wild-type RF1 (Figure 2).

The transient-state kinetics of RF1 binding showed a biphasic fluorescence change and, with the concentration dependence profiles described above, can be interpreted as a second-order association step followed by a first-order conformational change (*16*). However, other binding mechanisms may also result in biphasic kinetics such as subpopulations of either binding partner or multiple binding pathways. If subpopulations of RF1 binding to the ribosome are responsible for the biphasic kinetics, we would expect the amplitude of the second phase to decrease as the concentration of RF1 is increased because the faster binding population of RF1 would quickly occupy all available binding sites. Therefore, the constant amplitudes in the case of wild-type RF1 support a two-step binding mechanism. The biphasic fluorescence change observed in the case of H197A RF1 is also consistent with a two-step binding mechanism due to the correlation between the calculated affinity of the first binding step and the concentration dependence of the amplitude of the first phase.

The kinetic data show that the association rate constants (k_1) are similar for wild-type and H197A RF1. By contrast, the dissociation rate constant is at least 1000-fold faster for H197A RF1 ($k_{-1} < 0.1$ s^{-1} for wild-type RF1, and $k_{-1} = 175$ s^{-1} for H197A RF1) (Figure 3). Interestingly, the dissociation rate constant of H197A RF1 is similar to the value obtained with wild-type RF1 binding to a sense codon in the decoding center ($k_{-1} = 25-350$ s^{-1}) (*7*). His 197 in RF1, therefore, is clearly essential for the initial binding interaction with the ribosome. It is possible that the stacking interaction of the second base of the stop codon with His 197 triggers conformational changes in the decoding center that locks the RF on the ribosome.

The time course of RF1 binding to the ribosome showed a second, slow phase that is independent of the concentration of RF1. This is consistent with a first-order conformational change following the RF1 association step. The rates for the second phase (k_2) are similar for wild-type and H197A RF1, indicating that H197 is not essential for this conformational change. The saturation rate of 1 s^{-1} for the second phase is comparable to the rate of peptide release by RF1, suggesting it is rate-limiting for peptide release. The second phase may be monitoring the switch into the more tightly bound final conformation. However, the final conformation attained by H197A RF1 has a 100-fold lower binding affinity than wild-type RF1. This can be partially explained by the loss of favorable stacking interactions with the second base of the stop codon, the inhibition of conformational changes in the decoding center that overcomes the steric clash by A1913 of 23S rRNA, the global misalignment of H197A RF1 on the ribosome, or a combination of these factors.

The rate of peptide release is 5-fold slower with H197A RF1 than with wild-type RF1 (Figure 4A). This lower rate of peptide release is not due to weakened binding of H197A RF1 because these experiments were performed with saturating amounts of H197A RF1. The most likely explanation is that H197A RF1 is not correctly bound to the decoding center of the ribosome. This may cause the rest of the H197A RF1 to become misaligned, especially the universally conserved GGQ motif that is essential for peptide release. These interpretations are consistent with a previous study indicating that the GGQ motif of RF1 may be misaligned because of poor docking in the decoding center (*17*). More recent structure probing studies have shown that a sense codon in the decoding center can cause RF1 to become incorrectly positioned in the ribosome (*18*). Here we have kinetically revealed a link between decoding center interactions and peptide release by RF1. Interestingly, the rate of peptide release is

inhibited by 100−1000-fold with a sense codon (*7*); by contrast, the relatively modest defect in peptide release by H197A RF1 indicates that the overall arrangement of H197A RF1 on the ribosome is still somewhat similar to that of wild-type RF1.

In summary, our studies quantitatively evaluated the role of the highly conserved H197 in RF1 binding to the ribosome and the catalysis of peptide release. Our results show that H197 is critical for the binding step and significant for peptidyl-tRNA hydrolysis. In addition, we show that after the initial binding of H197A RF1 to the ribosome, a conformational switch occurs to a more tightly bound state (Figure 4B). Quantitatively determining the role of other residues in RF1 and RF2 for stop codon recognition and catalysis of peptide release is essential for mechanistically understanding how these protein factors achieve their high fidelity during translation termination.

ACKNOWLEDGMENT

We thank Jack Kyte for discussions and Ulrich Muller for comments on the manuscript.

REFERENCES

1. Brenner, S., Stretton, A. O., and Kaplan, S. (1965) Genetic code: The 'nonsense' triplets for chain termination and their suppression. *Nature 206*, 994–998.
2. Scolnick, E., Tompkins, R., Caskey, T., and Nirenberg, M. (1968) Release factors differing in specificity for terminator codons. *Proc. Natl. Acad. Sci. U.S.A. 61*, 768–774.
3. Konecki, D. S., Aune, K. C., Tate, W., and Caskey, C. T. (1977) Characterization of reticulocyte release factor. *J. Biol. Chem. 252*, 4514–4520.
4. Capecchi, M. R. (1967) Polypeptide chain termination in vitro: Isolation of a release factor. *Proc. Natl. Acad. Sci. U.S.A. 58*, 1144–1151.
5. Jorgensen, F., Adamski, F. M., Tate, W. P., and Kurland, C. G. (1993) Release factor-dependent false stops are infrequent in *Escherichia coli*. *J. Mol. Biol. 230*, 41–50.
6. Freistroffer, D. V., Kwiatkowski, M., Buckingham, R. H., and Ehrenberg, M. (2000) The accuracy of codon recognition by polypeptide release factors. *Proc. Natl. Acad. Sci. U.S.A. 97*, 2046–2051.
7. Hetrick, B., Lee, K., and Joseph, S. (2009) Kinetics of stop codon recognition by release factor 1. *Biochemistry 48*, 11178–11184.
8. Ito, K., Uno, M., and Nakamura, Y. (2000) A tripeptide 'anticodon' deciphers stop codons in messenger RNA. *Nature 403*, 680–684.
9. Laurberg, M., Asahara, H., Korostelev, A., Zhu, J., Trakhanov, S., and Noller, H. F. (2008) Structural basis for translation termination on the 70S ribosome. *Nature 454*, 852–857.
10. Weixlbaumer, A., Jin, H., Neubauer, C., Voorhees, R. M., Petry, S., Kelley, A. C., and Ramakrishnan, V. (2008) Insights into translational termination from the structure of RF2 bound to the ribosome. *Science 322*, 953–956.
11. Korostelev, A., Asahara, H., Lancaster, L., Laurberg, M., Hirschi, A., Zhu, J., Trakhanov, S., Scott, W. G., and Noller, H. F. (2008) Crystal structure of a translation termination complex formed with release factor RF2. *Proc. Natl. Acad. Sci. U.S.A. 105*, 19684–19689.
12. Bartetzko, A., and Nierhaus, K. H. (1988) Mg^{2+}/NH_4^+/polyamine system for polyuridine-dependent polyphenylalanine synthesis with near in vivo characteristics. *Methods Enzymol. 164*, 650–658.
13. Powers, T., and Noller, H. F. (1991) A functional pseudoknot in 16S ribosomal RNA. *EMBO J. 10*, 2203–2214.
14. Studer, S. M., Feinberg, J. S., and Joseph, S. (2003) Rapid Kinetic Analysis of EF-G-dependent mRNA Translocation in the Ribosome. *J. Mol. Biol. 327*, 369–381.
15. Feinberg, J. S., and Joseph, S. (2006) A conserved base-pair between tRNA and 23 S rRNA in the peptidyl transferase center is important for peptide release. *J. Mol. Biol. 364*, 1010–1020.
16. Johnson, K. A. (1992) Transient-state kinetic analysis of enzyme reaction pathways. In The Enzymes (Sigman, D. S., Ed.) pp 1−61, Academic Press, Inc., New York.
17. Youngman, E. M., He, S. L., Nikstad, L. J., and Green, R. (2007) Stop codon recognition by release factors induces structural rearrangement of the ribosomal decoding center that is productive for peptide release. *Mol. Cell 28*, 533–543.
18. He, S. L., and Green, R. (2010) Visualization of codon-dependent conformational rearrangements during translation termination. *Nat. Struct. Mol. Biol. 17*, 465–470.
19. Sund, J., Ander, M., and Aqvist, J. (2010) Principles of stop-codon reading on the ribosome. *Nature 465*, 947–950.